Food Innovation and Advances

ARTICLE

Open Access

https://doi.org/10.48130/fia-0025-0011

Food Innovation and Advances **2025**, 4(1): 108–115

Extraction of triterpenoids from *Carya cathayensis* Sarg. husks and enhancement of their antibacterial properties by loading into chitosan aerogels

Haixin Sun[1], Xinya Gu[1], Baozhu Shi[1], Tianhua Huang[2], Junlai Nian[2], Jidong Sun[2], Tarun Belwal[3], Liezhou Zhong[4], Benu Adhikari[5] and Zisheng Luo[1*]

[1] *College of Biosystems Engineering and Food Science, Zhejiang University, Hangzhou 310058, Zhejiang,China*
[2] *Qingdao CIMC Special Reefer Co., Ltd, Qingdao 266318, Shandong, China*
[3] *7 Continents Natural Products LLC, New Jersey, 500049, USA*
[4] *Nutrition & Health Innovation Research Institute, School of Medical and Health Sciences, Edith Cowan University, Joondalup, Western Australia, 6027, Australia*
[5] *School of Science, RMIT University, Melbourne, VIC 3083, Australia*
* Corresponding author, E-mail: luozisheng@zju.edu.cn

Abstract

Carya cathayensis Sarg. is widely cultivated in China as a specialized nut crop, and its discarded husks (outer pericarp) are rich in triterpenoids with known antibacterial properties. In this study, triterpenoids were extracted from *Carya cathayensis* Sarg. husks (CCSHs) using a surfactant-mediated, ultrasound-assisted extraction method optimized via response surface methodology, the optimized extraction yield was 33.92 ± 0.52 mg UAE/g DW. Ab-8 macroporous resin was used to purify the triterpenoids from the crude extracts, achieving a 4.3-fold increase in purity. Mesoporous chitosan aerogels were prepared, and their morphology, pore size, and specific surface area were evaluated using microscopic and nitrogen adsorption methods. These aerogels were then used to adsorb the purified triterpenoids from CCSH extracts, enhancing their antibacterial effect. Growth curves of *Escherichia coli* and *Staphylococcus aureus* demonstrated that the combination of CCSHs-derived triterpenoids and chitosan aerogel spheres resulted in an enhanced antibacterial effect. This study lays the groundwork for adding value to CCSHs while offering a pathway to develop plant-based antibacterial products.

Citation: Sun H, Gu X, Shi B, Huang T, Nian J, et al. 2025. Extraction of triterpenoids from *Carya cathayensis* Sarg. husks and enhancement of their antibacterial properties by loading into chitosan aerogels. *Food Innovation and Advances* 4(1): 108–115 https://doi.org/10.48130/fia-0025-0011

Introduction

Carya cathayensis Sarg. (Chinese hickory), hereafter referred to as *C. cathayensis,* is a tree species within the genus Juglans of the family Juglandaceae, predominantly distributed in the Zhejiang and Anhui provinces of China[1]. The kernel of *C. cathayensis* is rich in beneficial lipids and polyphenols, making it highly nutritious[2], therefore, it is produced in large quantities as a special agricultural product in Zhejiang province (China). However, large-scale kernel production generates a substantial quantity of discarded exocarps annually. The fibrous exocarp, an organic by-product, contains a large amount of cellulose, alkaloids, and triterpenoids[3], is difficult to degrade naturally, and presents significant opportunities for valorization. Triterpenoids have received extensive attention in recent years due to their excellent antibacterial and other physiological activities. Several triterpenoids, such as ursolic acid, hawthorn acid, and betulinic acid, exhibit the potential for antibacterial and antifungal applications[4,5]. Compared to conventional antibiotics, triterpenoids derived from natural sources are considered safer, making them a promising alternative for addressing antibiotic resistance[6]. However, studies on the triterpenoid content and characteristics of CCSHs remain limited, despite their significance. Therefore, studying the extraction, quantification, and potential applications of triterpenoids from CCSHs is highly significant.

Ultrasound-assisted extraction is a safe and efficient method that employs cavitation and thermal effects to physically disrupt plant cells within a short timeframe, facilitating cell rupture and the release of intracellular contents[7]. Due to its ability to enhance the release of bioactive substances and reduced extraction time, ultrasound-assisted extraction is considered an environmentally friendly and energy-efficient approach for large-scale production of plant-based ingredients. Surfactants like Span and Tween, commonly used in food processing, are known to lower surface tension and improve solvent penetration, further enhancing the extraction process[8]. The synergy between ultrasound waves and surfactants enables more effective disruption of the plant cell walls, which is crucial for improving the yield and quality of extracted phytochemicals. Recent studies have demonstrated that combining ultrasound-assisted extraction with non-ionic surfactants results in higher concentrations of desired bioactive compounds, such as polyphenols[9], flavonoids[10], and essential oils[11], compared to traditional extraction methods.

Triterpenoids, which possess a 30-carbon skeleton and a ring structure, are highly hydrophobic and only dissolve in non-polar organic solvents[12]. The hydrophobicity of triterpenoids makes their dissolution and encapsulation challenging, thereby limiting their practical use including in antimicrobial applications. Aerogel, a material with a highly porous structure, is formed by removing the liquid phase from a gel network and is characterized by abundant three-dimensional channels and exceptionally high porosity, typically exceeding 80%[13]. These features give aerogel excellent adsorption properties, allowing it to adsorb triterpenoid compounds. Chitosan, a biocompatible polysaccharide with multiple functional groups, shows great potential in the biological field as an antimicrobial agent and antioxidant[14]. Chitosan's cationic amino groups electrostatically interact with the anionic groups of bacterial cell walls, thereby inhibiting bacterial growth and reproduction[15]. Therefore, aerogel particles prepared by chitosan can not only

improve the application effect of poorly soluble antibacterial substances but also further enhance the antibacterial effect. Previous studies have shown that chitosan aerogels can produce synergistic antibacterial effects with compounds such as curcumin[16], and vancomycin[17]. However, the potential synergistic antimicrobial effects of triterpenoid-loaded chitosan aerogels remain underexplored.

In this study, surfactants and ultrasound were combined to extract triterpenoids from CCSHs, and the response surface method was employed to optimize the total triterpenoid extraction process. To address the poor water solubility of triterpenoids, porous chitosan aerogel spheres were developed for their adsorption. The feasibility of adsorption was evaluated and the adsorption capacity and structural properties of chitosan aerogel spheres were characterized using advanced techniques. Microbial growth curves were further analyzed to investigate the antimicrobial properties of the chitosan aerogel spheres before and after adsorbing triterpenoid extracts. This work addresses the limited exploration of CCSHs-derived triterpenoids, proposes their novel application via chitosan aerogel adsorption, and demonstrates their potential antibacterial activity.

Materials and methods

Material and chemicals

The semi-dried *Carya cathayensis* Sarg. husks (CCSHs) were collected from the farm in Hangzhou, Zhejiang province, China. The husks were washed with distilled water and dried at 35 °C for 24 h before being ground into powder[18].

Luria-Bertani broth was purchased from Sangon Biotech Co., Ltd. (Shanghai, China). AB-8 macroporous resin was purchased from Beijing Solarbio Science & Technology Co., Ltd. (Beijing, China). All other chemicals used were of analytical grade and purchased from Aladdin Reagent Co., Ltd. (Shanghai, China).

Analysis of total triterpenoid content

Total triterpenoid content was determined by vanillin-glacial acetic acid chromogenic method[19] with slight modifications, the ursolic acid standard curve was plotted for calculating the content of triterpenoid. Briefly, 500 μL of freshly made vanillin-glacial acetic acid solution (5%, w/v) and 800 μL of perchloric acid were added to the triterpenoid solution. The mixture was incubated at 65 °C for 15 min. Then 5 mL of glacial acetic acid was added to dilute the incubated solution to terminate the reaction. The absorbance was measured at 550 nm, and the extraction yield was expressed as milligrams of ursolic acid equivalents per gram dry weight of CCSHs (mg UAE/g DW).

Optimization of triterpenoid extraction

Single factor experiments of ultrasound-assisted surfactant extraction

The triterpenoids of CCSHs were extracted using a solvent containing 75% ethanol and Span-80. The extraction process was assisted using 300 W ultrasound. The effects of surfactant concentration (0, 1.4%–2.2% v/v), extraction temperature (20–60 °C), extraction time (10–50 min), and solvent to solid ratio (20–60 mL/g) on the total extraction yield were determined.

Response Surface Methodology (RSM) design

Design-Expert 11 (State-Ease Inc., Minneapolis, MN, USA) was used to optimize the yield of total triterpenoids from CCSHs. A three-factor, three-level Box-Behnken design (BBD) based on single-factor experiments was used for experimental design, modeling, and analysis.

Triterpenoid purification using macroporous resin

AB-8 macroporous resin with good triterpenoid adsorption was selected, and the preparation of macroporous resin was referenced to the method of Guo et al.[20], pure macroporous resin was packed into a chromatography column, the CCSH extract was loaded onto the column, allowed to adsorb for 2 h, and the liquid was drained. The CCSH extracts absorbed on the column were sequentially rinsed with deionized water, followed by 25%, 50%, and 75% ethanol. The 75% ethanol eluate was collected, and the concentration of triterpenoid extract was determined. The triterpenoid extracts, both before and after purification, were frozen at −80 °C for 12 h and then freeze-dried for 36 h. The lyophilized samples were dissolved in 70% methanol, centrifuged, and the supernatant was collected for purity testing.

Preparation of chitosan aerogel microspheres

Chitosan aerogel spheres were prepared as described by Li et al.[21]. Briefly, chitosan was dissolved in 1% glacial acetic acid solution (w/v) by stirring until a yellow gel was formed. Sonication at 80 Hz was performed to remove bubbles and the insoluble chitosan was filtered out. Chitosan gel droplets gelatinized in an acidic environment and quickly solidified into spherical particles when transferred to an alkaline solution (1 mol/L NaOH), and the spheres were hardened for 1 h and washed with deionized water. The microspheres were snap frozen using liquid nitrogen and then vacuum freeze dried for 24 h.

Acquiring surface morphology

The overall shape and morphology of the dried aerogel spheres were observed using a Gemini560 scanning electron microscope (ZEISS, DEU). An accelerating voltage of 15.0 kV was used for this purpose.

Specific surface area and pore size

The surface area and pore structure of the aerogel spheres were characterized using the gas adsorption method based on capillary condensation, with measurements taken by the TriStar II Plus (Micromeritics, USA) using nitrogen (N_2) as the adsorption gas[22]. Isothermal adsorption-desorption curves were generated by measuring the volume of gas adsorbed and desorbed at various relative pressures.

Determination of adsorption capacity

Chitosan aerogel spheres (40 mg) were immersed in an ethanol solution containing triterpenoid extracts at a concentration of 1 mg/mL and shaken at 120 rpm for 10 h to facilitate triterpenoids absorption. The formulae for calculating the adsorption capacity (q_t) and adsorption rate (R_a) are as follows:

$$q_t\ (\mathrm{mg/g}) = \frac{C_0V_0 - C_tV_t}{m} \quad (1)$$

$$R_a\ (\%) = \frac{C_0 - C_t}{C_0} \quad (2)$$

where, C_0, V_0: initial concentration and volume of triterpenoids solution; C_t, V_t: concentration and volume of the solution following sampling.

FTIR analysis of triterpenoids and triterpenoid-loaded chitosan aerogels

The functional groups of the triterpenoid-loaded chitosan aerogel spheres and the triterpenoid extracts were analyzed using a Fourier transform attenuated total reflection infrared (ATR-FTIR) spectrometer (Nicolet iS50FT-IR, Thermo Scientific, USA).

Thermal stability analysis

The thermal gravimetric analyzer (TGA, METTLER TOLEDO, Switzerland) was used to investigate the weight loss of chitosan

aerogel spheres during heating both without and with triterpenoids adsorption. The thermogravimetric (TG) curve was obtained by increasing the temperature from 30 to 800 °C at a rate of 10 °C per min under a N_2 atmosphere[23]. The derivative of the TG curve (DTG) was obtained by differentiation.

Antibacterial capacity analysis

E. coli and *S. aureus*, two common microorganisms that cause gut microbial infections and food poisoning[24], were selected in the logarithmic growth phase and dissolved in Luria-Bertani medium, shaken at 180 rpm at 37 °C for 12 h. This bacterial suspension was diluted to 10^4 cfu/mL. Then, 40 mg of chitosan aerogel spheres with or without triterpenoids adsorption and some extract powder with an amount comparable to chitosan adsorbed triterpenoids were added to the bacterial suspension, individually[25]. The chitosan aerogel spheres without triterpenoids loading were also soaked in ethanol and dried under the conditions mentioned above. The optical density (OD_{600}) was measured at 0, 1, 2, 4, 6, 8, 10, 12, and 24 h to plot the microbial growth curve. Medium without chitosan aerogel was used as a control.

Statistical analysis

Experiments were conducted in triplicate unless specified otherwise. The data are presented as the mean ± standard deviation (SD), with statistical analysis performed using one-way ANOVA and Tukey's test at a 95% confidence level ($p < 0.05$).

Results and discussion

Single-factor extraction experiments

The results of these experiments are presented in Fig. 1 and Supplementary Table S1. The data in Supplementary Table S1 confirmed that Span-80 effectively increased the extraction yield of total triterpenoids from CCSHs. The yield of total triterpenoids increased as the concentration of Span-80 rose within the range of 1.4% to 2%. A maximum yield of 19.9 ± 0.25 mg UAE/g DW was achieved at a Span-80 concentration of 2% (Fig. 1a), while concentrations below 1.4% showed no significant difference in yield (not more than 17.56 ± 0.33 mg UAE/g DW) compared to the control. As the surfactant concentration increased, the number of surfactant molecules in solution also increased, leading to the formation of micelles, which interacted with ultrasound, which enhanced the extraction process[26,27]. However, a significant decrease ($p < 0.05$) in yield was observed when the surfactant concentration exceeded 2%, consistent with findings from other studies on polyphenols using ultrasound-assisted aqueous extraction[28]. This reduction in extraction yield can be attributed to the saturation of micelles, which could no longer interact with additional triterpenoids effectively, as well as the increased viscosity of the solution, which interferes with mass transfer[29], leading to a decrease in extraction efficiency.

When ultrasound at 300 W power level was applied, the extraction efficiency of total triterpenoids showed an increasing trend as the temperature increased from 20 to 50 °C (Fig. 1b). This phenomenon can be attributed to the reduction in solution viscosity with a moderate increase in temperature, which enhances solute diffusion. Moderately high temperatures also render plant cells more susceptible to swelling and rupture, facilitating the release of compounds[30]. However, excessive heating can lead to decomposition or denaturation of triterpenoids[31], as evidenced by the decreased yield at 60 °C. A similar decrease in triterpenoid yield at elevated temperatures has been reported[19]. Furthermore, higher temperatures may disrupt the formation and stability of ultrasonic

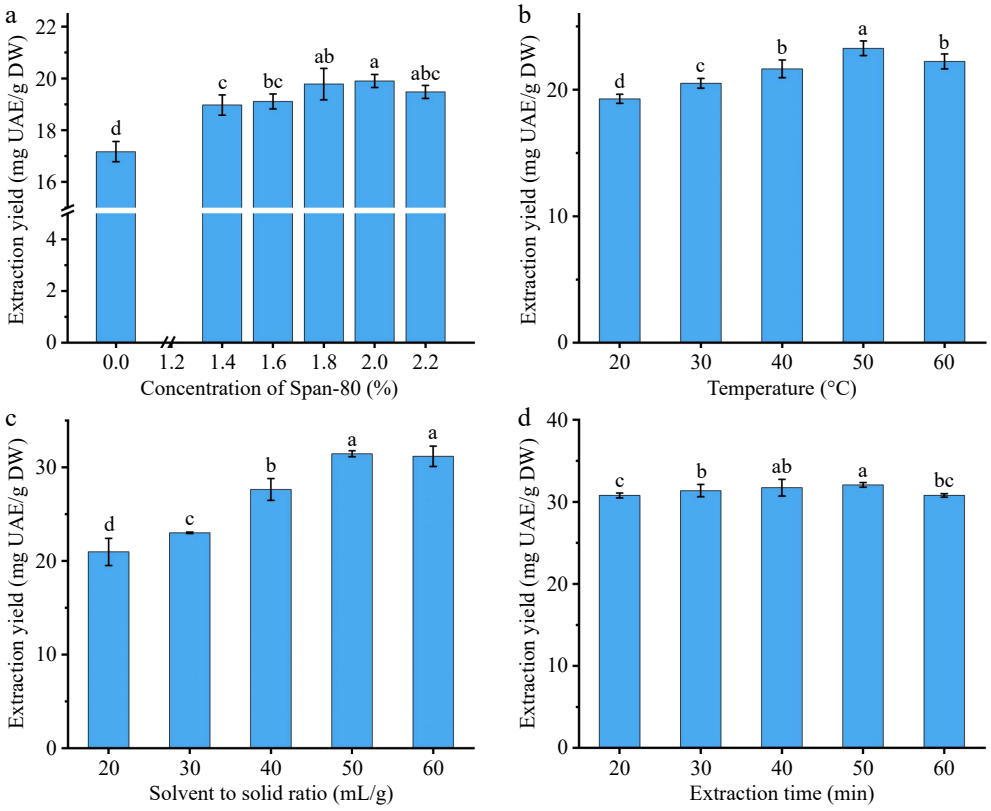

Fig. 1 Effects of (a) surfactant concentration, (b) temperature, (c) solvent to solid ratio, and (d) extraction time on the extraction yield of total triterpenoids.

cavitation bubbles, thereby reducing the efficiency of the ultrasound-assisted extraction method[32].

For a given solid mass of raw material, increasing the solvent-to-solid ratio improved the extraction efficiency, achieving a maximum yield of 31.44 ± 0.31 mg UAE/g DW at a ratio of 50 mL/g (Fig. 1c). Initially, the increased solvent volume provided greater solvation power (higher concentration gradient and increased contact between the solids and the solvent), which promoted the transfer of triterpenoids from the raw material into the solvent. However, exceeding the optimal solvent-to-solid ratio resulted in over-cavitation that disrupted the target triterpenoids and ultimately reduced the yield[28].

The cavitation effect of ultrasound is vital for enhancing extraction. As cavitation bubbles form and collapse, they generate localized heat and pressure, causing the rupture, erosion, shearing, and swelling of plant cell structures[28]. These effects promote substance dissolution in the early stages, but prolonged cavitation can degrade target compounds, ultimately reducing extraction efficiency, as shown in Fig. 1d.

Optimization for the extraction of triterpenoids

The response surface plots and the corresponding contour plots are shown in Fig. 2. The total triterpenoid yield under various combinations of extraction conditions A: extraction temperature, B: extraction time, and C: solvent to solid ratio, was represented by the response surface Eqn (3).

$$Y = 32.31 + 0.65A + 0.50B + 1.53C + 0.79AC + 0.61BC - 1.49B^2 - 2.03C^2 \quad (3)$$

The BBD experimental design, incorporating different combinations of factors, and their predicted and actual values are presented in Supplementary Table S2. The ANOVA results, shown in Supplementary Table S3, indicate that all coefficients, except A^2 and AB, had a significant impact on the extraction yield ($p < 0.05$). The p-value of the fitting model was less than 0.001, and the correlation between predicted and experimental values is illustrated in Supplementary Fig. S1.

Based on the regression model, the optimal extraction conditions were found to be: 65 °C, 42 min with a solvent-to-solid ratio of 58 mL/g. The predicted maximum extraction yield was 34.01 mg UAE/g DW, and the experimental maximum yield was 33.92 ± 0.52 mg UAE/g DW. These findings show that the quadratic model realistically predicted the extraction yield of triterpenoids.

Purification of triterpenoids

The crude CCSHs triterpenoid extracts were adsorbed onto AB-8 macroporous resin and eluted with ethanol, yielding a tan-colored lyophilized powder with a purity of 56.6%, a 4.3-fold improvement. The purified triterpenoids were then used for chitosan aerogel adsorption experiments.

Surface morphology of chitosan aerogel spheres

The hydrophobicity of triterpenoids weakens their antibacterial activity. To improve their antimicrobial activity, chitosan aerogel spheres were prepared to adsorb triterpenoids from CCSHs. SEM was used to examine the topography and pore distribution of the chitosan aerogel spheres. SEM images revealed less structural collapse in the 3 wt% chitosan gel after freeze-drying (Fig. 3a, e) compared to the 2.5 wt% chitosan gel. They also revealed a surface with multiple pores and a well-defined network structure of 3 wt% chitosan gel (Fig. 3b, c). This difference in surface morphology can be attributed to the lower concentration of chitosan in the 2.5 wt% gel, which was less robust and could not resist structural collapse during the lyophilization process. In contrast, the higher chitosan concentration (3 wt%) facilitated better cross-linking among molecular chains, including hydrogen bonding and other interactions, reinforcing the molecular framework and forming a stable, three-dimensional structure with a uniform porous network[21]. Based on these findings, subsequent experiments focused on optimizing the adsorption properties of the 3 wt% chitosan aerogel spheres.

Characterization of the chitosan aerogels

Gas adsorption is commonly used to characterize porous materials. This method involves adsorbing N_2 onto adsorbent particles at 77 K, and then desorbing the N_2 by heating the sample[33]. This method enables the determination of the specific surface area and categorizes the pore size distribution during the adsorption-desorption cycle. When characterizing porous materials, various computational methods are used to determine a material's structural characteristics.

Brunauer-Emmett-Teller (BET) analysis determined the micropores and mesopores, while Barrett-Joyner-Halenda (BJH) determined the mesopores and macropores[21]. At $p/p_0 = 0.953$, the total pore volume was 0.108 cm^3/g (BET) and 0.085 cm^3/g (BJH). The average pore sizes were 3.99 nm (BET) and 3.48 nm (BJH), and the specific surface area was 97.1 m^2/g (BJH). These results confirm the mesoporous structure of the chitosan aerogel spheres. The large specific surface area and porous internal structure of the chitosan aerogel spheres are vital for their adsorption capacity.

According to the method mentioned above, the adsorption capacity of chitosan aerogel spheres for triterpenoids is 123.5 ± 0.71 mg/g, and the adsorption rate is 19.9% ± 0.20%.

Additionally, the functional groups present on the chitosan surface enable interactions with adsorbed substances through chemical bonding or physical forces, further contributing to their adsorption performance. As shown in Fig. 4a, the infrared spectrum of chitosan aerogel (CA) shows a peak at 3,362 cm^{-1}, which is a result of the overlapping stretching vibrations of the O-H and N-H bonds in the chitosan molecule[34]. The peak appears at 2,876 cm^{-1} representing the symmetric stretching vibration of the C-H bond[35]. The peaks at 1,592 cm^{-1} and 1,150 cm^{-1} correspond to the N-H bending and C-O-C bending vibrations, respectively, indicating the presence of amide groups in chitosan[36]. The peak that appears at 1,059 cm^{-1} corresponds to the stretching vibration of the C-O bond, which is indicative of the amino and hydroxyl groups. Interestingly the peak that typically appears at 1,650 cm^{-1} representing C=O stretching vibration was absent. This absence could be due to the crystalline structure formed during the preparation of the aerogel.

In the infrared spectrum of the CCSHs triterpenoids, the peaks appear at 3,351 and 1,607 cm^{-1} correspond to O-H stretching and C=O stretching vibrations, respectively. The peak at 1,104 cm^{-1} is likely due to the C-O-C stretching vibration. When comparing the infrared spectrum of chitosan aerogel (CA) with that of chitosan aerogel adsorbed with the CCSHs extracts (CCA), the O-H and N-H stretching vibration peak that appeared at 3,362 cm^{-1} in CA shifted to 3,356 cm^{-1} in CCA. Additionally, new peaks at 2,973 and 1,602 cm^{-1} appeared, while the peak at 1,059 cm^{-1} disappeared. These changes could be attributed to the formation of hydrogen bonds between the triterpenoids and the hydroxyl groups of chitosan.

The thermogravimetric (TG) curve (Fig. 4b) was used to describe the mass change of chitosan aerogel spheres during the heating process, while the derivative thermogravimetric (DTG) curve (Fig. 4c) represents the first-order differential of the thermogravimetric curve with respect to temperature. The weight loss curves of chitosan aerogel before and after adsorbing triterpenoids from the CCSH extracts were roughly similar and could be divided into four stages. The first stage (30–100 °C) corresponds to the evaporation of

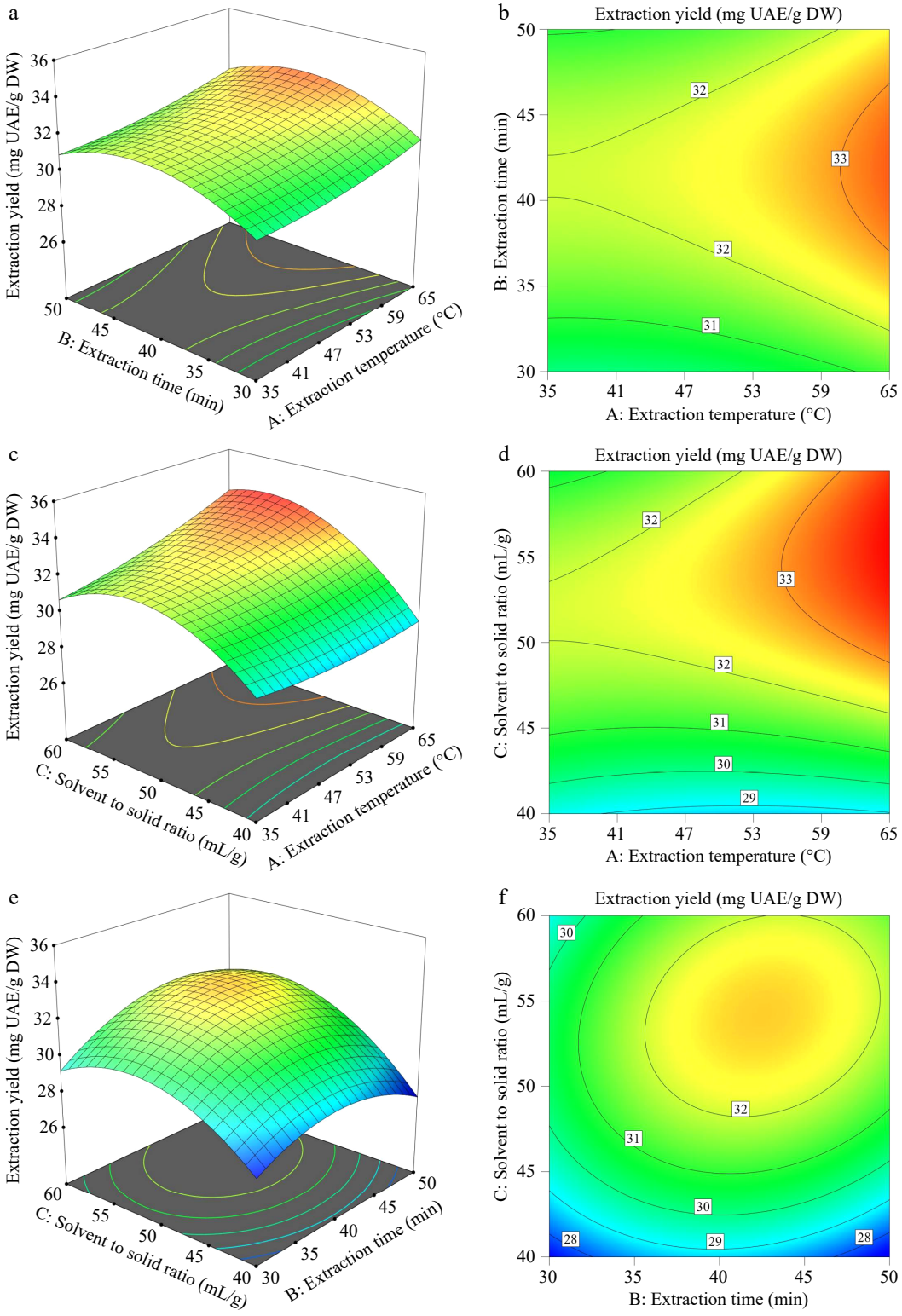

Fig. 2 (a), (c), (e) Response surface diagrams, and (b), (d), (f) the corresponding contour plots of the total triterpenoid yield.

adsorbed water, resulting in mass loss. In the second stage (100–250 °C), the material's mass remained constant. In the third stage (250–380 °C), chitosan began to degrade, and in the fourth stage (380–800 °C), chitosan was further carbonized and decomposed, resulting in additional mass loss. During these stages, chitosan underwent various reactions, including dehydration, deamination, and the breakage of glycosidic bonds, which are reflected in the mass changes as a function of temperature[37]. Aerogels loaded with the extracts exhibited less mass loss compared to unloaded chitosan, suggesting that the interaction between the extracts and the aerogel enhanced its thermal stability[38].

Antimicrobial activity

The growth curve (Fig. 5) method was used to investigate the effects of chitosan aerogel (CA), triterpenoid extracts, and chitosan aerogel adsorbed extracts (CCA) on the growth of *E. coli* (Fig. 5a) and

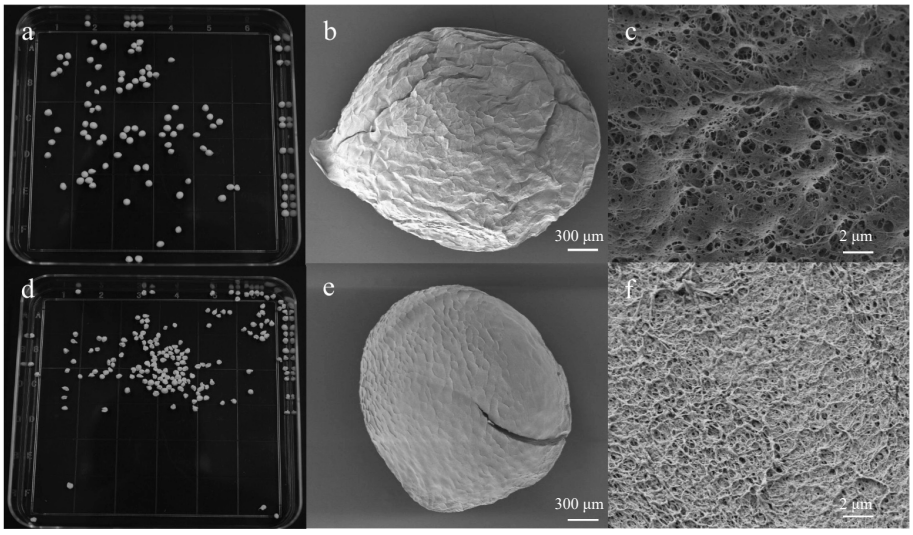

Fig. 3 The appearance, morphology, and surface pores observed by electron microscopy morphology of chitosan aerogel spheres prepared at the concentration of (a)–(c) 3 wt%, and (d)–(f) 2.5 wt%.

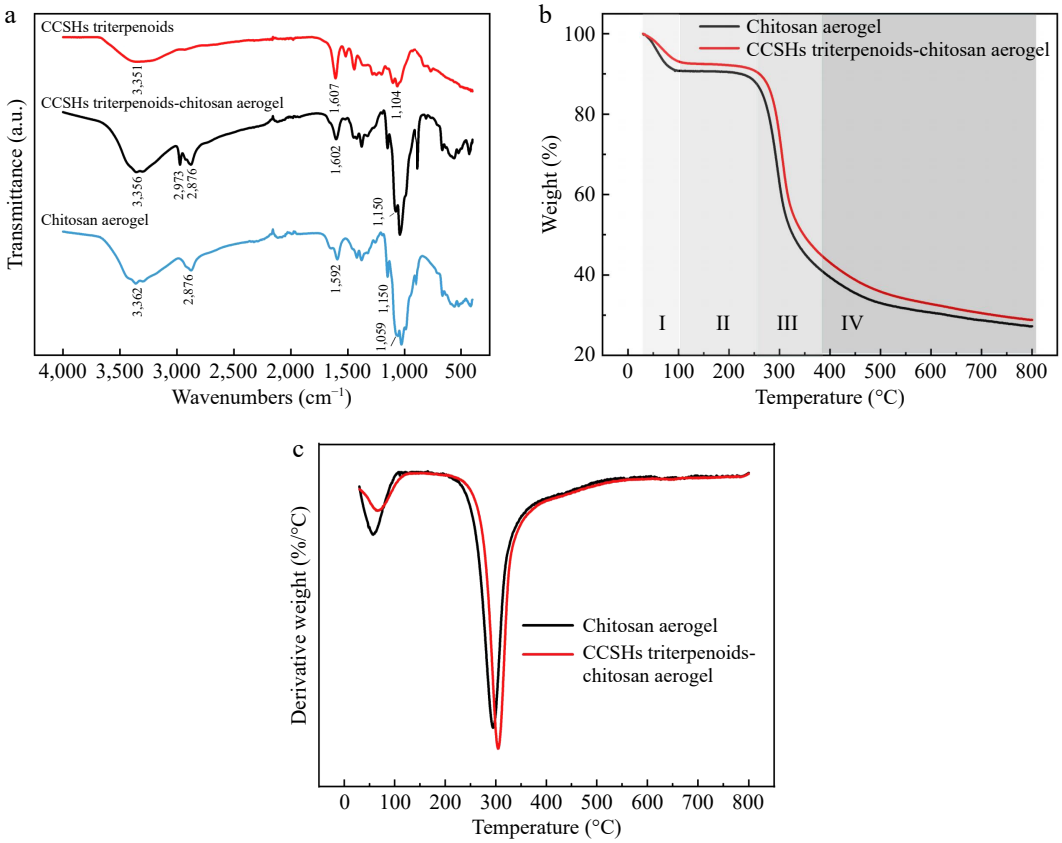

Fig. 4 (a) Fourier-transform infrared spectroscopy, (b) thermogravimetric curves, and (c) derivative thermogravimetry curves for chitosan aerogel spheres.

S. aureus (Fig. 5b) over a 24-h period. The OD_{600} value was used as an indicator of the growth density of microorganisms. Since most triterpenoid compounds were insoluble in water, these compounds exhibited weak antimicrobial effects. The results indicated that due to the adsorption of triterpenoids into chitosan aerogels, the water solubility of triterpenoids was improved, as shown by the lowest growth density. Both CA and CCA inhibited microbial growth, the growth density of the CCA group was lower than that of CA, indicating that chitosan aerogel and triterpenoids could achieve synergistic antibacterial effect.

E. coli entered the logarithmic growth phase within two hours of incubation at 37 °C. Its population density in the experimental groups was lower than in the control group, suggesting that triterpenoids and aerogel inhibited *E. coli's* growth rate. After 12 h, the *E. coli* population stabilized, with a slight decline observed. In contrast, *S. aureus* exhibited a longer lag phase, entering the logarithmic growth phase after 4 h, due to physiological differences

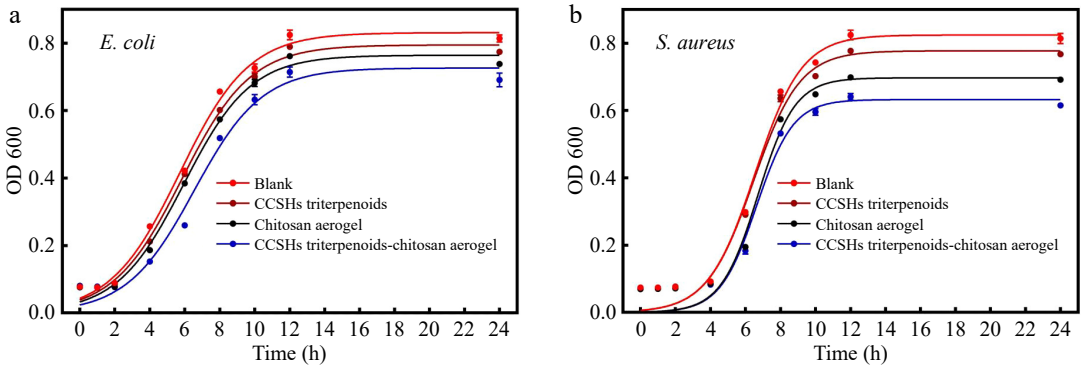

Fig. 5 Growth curves of (a) *E. coli,* and (b) *S. aureus.*

between the two strains, which has also been observed in other studies[39]. As shown in Fig. 5b, the growth density of *S. aureus* in the CCA and CA groups decreased more significantly than in the control group. In this experiment, *E. coli* exhibited a lower susceptibility to the antimicrobial effect of triterpenoids of CCSHs, which agrees with findings reported in other studies[38,40]. The teichoic acid in the cell walls and the complex membrane structure of gram-negative bacteria are reported to contribute to their stronger resistance to antimicrobial agents[41]. Additionally, the longer lag phase observed in *S. aureus* may have increased its sensitivity to environmental factors, resulting in a higher level of inhibition during this phase.

Overall, the results indicated that chitosan aerogel spheres loaded with the CCSH extracts exhibited better antibacterial properties. The combination of the two further inhibited microbial growth and reproduction, suggesting a synergistic effect. This improvement may be attributed to the ability of chitosan to increase the solubility of the triterpenoids[42].

Conclusions

An environmentally friendly non-ionic surfactant (Span-80) was combined with ultrasound-assisted extraction to extract triterpenoids from *Carya cathayensis* Sarg. husks (CCSHs), and the optimized triterpenoid yield was 33.92 ± 0.52 mg UAE/g DW. The chitosan aerogel spheres were characterized for their structure and porosity and employed to adsorb the triterpenoids purified by macroporous resin. The spheres loaded with CCSHs triterpenoids were tested for antimicrobial activity, and the growth curves of both *E. coli* and *S. aureus* indicated that the chitosan aerogel spheres absorbed the CCSHs triterpenoids exhibited a better antibacterial property against these two bacterial strains compared to using them alone. Future studies are expected to further refine this extraction method and conduct a more detailed analysis of the composition of the triterpenoids extracted from CCSHs. Overall, the combination of Span-80 and ultrasound-assisted extraction was proved to be a green and efficient method. The triterpenoids extracted from CCSHs hold great potential as plant-derived antimicrobial agents, provides a foundation to reduce processing waste from *Carya cathayensis* Sarg. and valorize CCSHs.

Author contributions

The authors confirm contribution to the paper as follows: conceptualization: Luo Z, Sun H, Gu X; methodology: Gu X; data curation, formal analysis and writing-original draft: Sun H; writing-review & editing: Shi B, Huang T, Nian J, Sun J, Belwal T, Zhong L, Adhikari B, Luo Z; funding acquisition and supervision: Luo Z.

Data availability

All data generated or analyzed during this study are included in this published article and its supplementary information files.

Acknowledgments

This research is funded by the Key Research and Development Program of Zhejiang Province (2023C02042), China.

Conflict of interest

The authors declare that they have no conflict of interest.

Supplementary information accompanies this paper at (https://www.maxapress.com/article/doi/10.48130/fia-0025-0011)

Dates

Received 26 December 2024; Revised 17 January 2025; Accepted 13 February 2025; Published online 12 March 2025

References

1. Xu L, Lu C, Zhou T, Wu J, Feng H. 2024. A 3D-2DCNN-CA approach for enhanced classification of hickory tree species using UAV-based hyperspectral imaging. *Microchemical Journal* 199:109981
2. Jiang C, Wang S, Wang Y, Wang K, Huang C, et al. 2024. Polyphenols from hickory nut reduce the occurrence of atherosclerosis in mice by improving intestinal microbiota and inhibiting trimethylamine N-oxide production. *Phytomedicine* 128:155349
3. Zhang J, Ying Y, Li X, Yao X. 2018. Evaluation of three kinds of nutshell with respect to utilization as culture media. *Bioresources* 13:7508–18
4. Ghanem DM, Okba MM, Ammar NM, Mohamed DA, El-Desoky AH, et al. 2024. *Genus Carissa* L.: a newly explored sustainable source of virulence inhibitors: a mini review. *Natural Product Research*
5. Khwaza V, Aderibigbe BA. 2024. Potential Pharmacological Properties of Triterpene Derivatives of Ursolic Acid. *Molecules* 29:3884
6. Chung PY, Navaratnam P, Chung LY. 2011. Synergistic antimicrobial activity between pentacyclic triterpenoids and antibiotics against Staphylococcus aureus strains. *Annals of Clinical Microbiology and Antimicrobials* 10:25
7. Fu X, Wang D, Belwal T, Xu Y, Li L, et al. 2021. Sonication-synergistic natural deep eutectic solvent as a green and efficient approach for extraction of phenolic compounds from peels of *Carya cathayensis* Sarg. *Food Chemistry* 355:129577
8. Karanth S, Iyyaswami R. 2021. Analysis of ionic and nonionic surfactants blends used for the reverse micellar extraction of Lactoperoxidase from whey. *Asia-Pacific Journal of Chemical Engineering* 16:e2590
9. Barar A, Bensebia O. 2025. Optimization of bioactive compounds recovery from thuya solid residues using ultrasound and nonionic

surfactants assisted extraction: A response surface methodology study. *Sustainable Chemistry and Pharmacy* 43:101878

10. Cui G, Liu B, Kang Y, Huang B, Yao L. 2024. Green surfactant and circulating ultrasound coupling extraction of total flavonoids from *Cynanchum auriculatum* leaves: parameter optimization, extraction mechanism, and HPLC-MS analysis. *Industrial Crops and Products* 222:119483
11. Wan N, Kou P, Pang HY, Chang YH, Cao L, et al. 2021. Enzyme pretreatment combined with ultrasonic-microwave-assisted surfactant for simultaneous extraction of essential oil and flavonoids from *Baeckea frutescens*. *Industrial Crops and Products* 174:114173
12. Chen L, Gong J, Yong X, Li Y, Wang S. 2024. A review of typical biological activities of glycyrrhetinic acid and its derivatives. *RSC Advances* 14:6557–97
13. Kuang J, Cai T, Dai J, Yao L, Liu F, et al. 2023. High strength chitin/chitosan-based aerogel with 3D hierarchically macro-meso-microporous structure for high-efficiency adsorption of Cu(II) ions and Congo red. *International Journal of Biological Macromolecules* 230:123238
14. Hong F, Qiu P, Wang Y, Ren P, Liu J, et al. 2024. Chitosan-based hydrogels: From preparation to applications, a review. *Food Chemistry: X* 21:101095
15. Ke CL, Deng FS, Chuang CY, Lin CH. 2021. Antimicrobial actions and applications of chitosan. *Polymers* 13:904
16. Wang F, Xu Z, Chen L, Qiao Z, Hu Y, et al. 2024. Super absorbent resilience antibacterial aerogel with curcumin for fresh pork preservation. *Food control* 159:110289
17. Yahya EB, Jummaat F, Amirul AA, Adnan AS, Olaiya NG, et al. 2020. A review on revolutionary natural biopolymer-based aerogels for antibacterial delivery. *Antibiotics* 9:648
18. Ettoumi FE, Zhang R, Belwal T, Javed M, Xu YQ, et al. 2022. Generation and characterization of nanobubbles in ionic liquid for a green extraction of polyphenols from Carya cathayensis Sarg. *Food Chemistry* 369:130932
19. Luo S, Zeng C, Luo F, Li M, Feng S, et al. 2020. Optimization of ultrasound-assisted extraction of triterpenes from Bergenia emeiensis leaves and inhibition effect on the growth of Hela cells. *Journal of Applied Research on Medicinal and Aromatic Plants* 18:100266
20. Guo L, Li X, Zhang J, Sun X, Li Y, et al. 2021. Optimization of extraction and macroporous resin purification processes of total triterpenoid from *Boletus edulis* Bull: Fr. *Journal of Food Processing and Preservation* 45:e15292
21. Li CG, Dang Q, Yang Q, Chen D, Zhu H, et al. 2022. Study of the microstructure of chitosan aerogel beads prepared by supercritical CO_2 drying and the effect of long-term storage. *RSC Advances* 12:21041–49
22. Liu Y, Zhang X, Shi J, Guo W, Kang L, et al. 2021. A reservoir quality evaluation approach for tight sandstone reservoirs based on the gray correlation algorithm: A case study of the Chang 6 layer in the W area of the as oilfield, Ordos Basin. *Energy Exploration & Exploitation* 39:1027–56
23. Sarmin SN, Jawaid M, Ismail AS, Hashem M, Fouad H, et al. 2023. Effect of chitosan filler on the thermal and viscoelasticity properties of bio-epoxy/date palm fiber composites. *Sustainable Chemistry and Pharmacy* 36:101275
24. Guo H, Zhao F, Lei B, Yang W, Guo L, et al. 2023. Synergistic antimicrobial system based on nisin and α-hydroxy organic acids. *Archives of Microbiology* 205:225
25. Gorshkova N, Brovko O, Palamarchuk I, Bogolitsyn K, Ivakhnov A. 2021. Preparation of bioactive aerogel material based on sodium alginate and chitosan for controlled release of levomycetin. *Polymers for Advanced Technologies* 32:3474–82
26. Feng W, Wang S, Duan X, Wang W, Yang F, et al. 2021. A novel approach for enhancing lipid recovery for biodiesel production from wet energy biomass using surfactants-assisted extraction. *Renewable Energy* 170:462–70
27. Kamiński J, Bujak P, Długosz M. 2024. Permeabilization of *Calendula officinalis* L. hairy root cultures for the release of accumulated triterpenoid saponins. *Plant Cell Tissue and Organ Culture* 159:5
28. Selvakumar P, Karthik V, Kumar PS, Asaithambi P, Kavitha S, et al. 2021. Enhancement of ultrasound assisted aqueous extraction of polyphenols from waste fruit peel using dimethyl sulfoxide as surfactant: assessment of kinetic models. *Chemosphere* 263:128071
29. Cui Q, Liu J, Xu W, Kang YF, Wang X, et al. 2019. Enhanced extraction and preconcentration of main target saponins from Panax notoginseng root using green and efficient formulated surfactant aqueous systems. *Journal of Cleaner Production* 210:1507–16
30. Yan MM, Liu W, Fu YJ, Zu YG, Chen CY, et al. 2010. Optimisation of the microwave-assisted extraction process for four main astragalosides in Radix Astragali. *Food Chemistry* 119:1663–70
31. Khoang LT, Huyen HTT, Chung HV, Duy LX, Toan TQ, et al. 2022. Optimization of total saponin extraction from polyscias fruticosa roots using the ultrasonic-assisted method and response surface methodology. *Processes* 10:2034
32. Hou M, Shi J, Lin C, Zhu L, Bian Z. 2024. Ultrasound-assisted extraction of triterpenoids from Chaenomeles speciosa leaves: Process optimization, adsorptive enrichment, chemical profiling, and protection against ulcerative colitis. *Ultrasonics Sonochemistry* 111:107136
33. Nazari MT, Schnorr C, Rigueto CVT, Alessandretti I, Melara F, et al. 2022. A review of the main methods for composite adsorbents characterization. *Environmental Science and Pollution Research* 29:88488–506
34. Ren L, Xu J, Zhang Y, Zhou J, Chen D, et al. 2019. Preparation and characterization of porous chitosan microspheres and adsorption performance for hexavalent chromium. *International Journal of Biological Macromolecules* 135:898–906
35. Kaczmarek H, Zawadzki J. 2010. Chitosan pyrolysis and adsorption properties of chitosan and its carbonizate. *Carbohydrate Research* 345:941–47
36. Xu J, Song W, Wu N, Tong J, Ren L. 2021. Preparation and characterization of chitosan/polyvinyl porous alcohol aerogel microspheres with stable physicochemical properties. *International Journal of Biological Macromolecules* 187:614–23
37. Pereira FS, da Silva Agostini DL, Job AE, González ERP. 2013. Thermal studies of chitin-chitosan derivatives. *Journal of Thermal Analysis and Calorimetry* 114:321–27
38. Hadidi M, Pouramin S, Adinepour F, Haghani S, Jafari SM. 2020. Chitosan nanoparticles loaded with clove essential oil: Characterization, antioxidant and antibacterial activities. *Carbohydrate Polymers* 236:116075
39. Tang M, Hao X, Kang Y, He X, Zhao H. 2024. Preparation and antibacterial properties of polyelectrolyte complexed nanoparticles aggregated from PHMG and Sodium Caffeate. *ACS Applied Bio Materials* 7:6467–76
40. Cai M, Wang Y, Wang R, Li M, Zhang W, et al. 2022. Antibacterial and antibiofilm activities of chitosan nanoparticles loaded with *Ocimum basilicum* L. essential oil. *International Journal of Biological Macromolecules* 202:122–29
41. Pan X, Junejo SA, Tan CP, Zhang B, Fu X, et al. 2022. Effect of potassium salts on the structure of gamma-cyclodextrin MOF and the encapsulation properties with thymol. *Journal of the Science of Food and Agriculture* 102:6387–96
42. Perinelli DR, Fagioli L, Campana R, Lam JKW, Baffone W, et al. 2018. Chitosan-based nanosystems and their exploited antimicrobial activity. *European Journal of Pharmaceutical Sciences* 117:8–20